CHEMISTRY
A EUROPEAN JOURNAL

DOI: 10.1002/chem.200701297

Synthesis, Characterisation, and In Vitro Evaluation of Pro^2-Ile^3-*S*-Deoxo-Amaninamide and Pro^2-D-*allo*-Ile^3-*S*-Deoxo-Amaninamide: Implications for Structure–Activity Relationships in Amanitin Conformation and Toxicity

Jonathan P. May, Pierre Fournier, Brian O. Patrick, and David M. Perrin*[a]

Abstract: The amatoxins are a family of toxic bicyclic peptides that inhibit RNA polymerase II. Herein we discuss an improved synthesis of these compounds from easily obtainable amino acids by means of a solid-phase methodology. Interestingly, we obtained two products of the same mass following our final macrocyclisation, relating to a similar distribution of products described in some previous reports. One of these products was the desired amatoxin; Pro^2-Ile^3-*S*-deoxo-amaninamide **1b**. The other compound, after thorough investigation, was confirmed to be the epimer Pro^2-D-*allo*-Ile^3-*S*-deoxo-amaninamide **1a**, not an atropisomer structure as previously suggested in syntheses of related amanitin analogues. Crystallographic data of **1a** confirms the presence of a βII-turn, rather than a βI-turn common to the natural toxin and **1b**. This difference explains the large variation in CD spectra, although it seems to have relatively little effect on the bioactivity in vitro. These data provide new insights into the bicyclic amatoxin structure.

Keywords: amatoxin · atropisomerism · circular dichroism · epimerization · peptides

Introduction

The bicyclic octapeptide α-amanitin (Figure 1), a natural toxin found in the fungus *Amanita phalloides*, is an exceptionally potent and highly selective inhibitor of eukaryotic RNA polymerase II ($K_d \approx 10^{-10}$ M).[1] Despite the extensive structural homology and evolutionary similarities between the large RNA polymerase subunits, amanitin is not an inhibitor for the bacterial RNA polymerases and only weakly inhibits pol I and pol III. Early synthetic studies showed that the bicyclic nature of amanitin provides rigidity, which is in turn responsible for amanitin's extraordinary potency towards RNA pol II; indeed, all three *seco*-peptides were largely inactive.[1]

The synthetic assembly of an amatoxin bicycle is accomplished by means of a backbone cyclisation and formation of a tryptathionine linkage between the side chains of tryptophan and cysteine. There has been significant investigation into the formation of this linkage and application to the synthesis of amanitin analogues. Zanotti et al. first described the synthesis of such compounds from the linear octapeptide followed by cross-linking and cyclisation.[2,3] This methodology utilised the Savige–Fontana reaction,[4–7] which required incorporation of a trityl protected cysteine and introduction of an Hpi (3a-hydroxypyrrolo[2,3-*b*]indole) moiety at the N terminus of the polypeptide chain.[7] Hence, subsequent deprotection of Cys(Tr) and activation of the Hpi with acid gave the desired tryptathionine linkage.

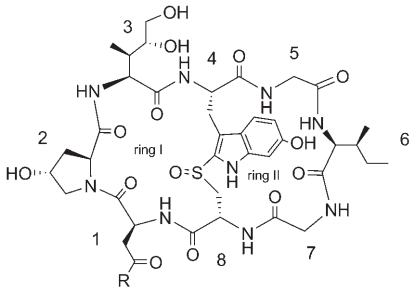

Figure 1. Structure of α-amanitin (R = NH_2) and β-amanitin (R = OH). Residues are numbered from 1–8.

Over the past 30 years, in excess of 40 amatoxins (synthetic, naturally occurring and derivatised) have been investigated to establish the extent to which various hydroxylated amino acid side chains contribute to toxicity.[2,3,8–14] These

[a] Dr. J. P. May, P. Fournier, Dr. B. O. Patrick, Prof. D. M. Perrin
Department of Chemistry, University of British Columbia
2036 Main Mall, Vancouver, BC V6T 1Z1 (Canada)
Fax: (+1) 604-822-2847
E-mail: dperrin@chem.ubc.ca

Supporting information for this article is available on the WWW under http://www.chemeurj.org/ or from the author.

studies showed that the 6-hydroxyindole and the sulfoxide could be replaced by just a simple tryptathionine, with minimal loss of activity. The hydroxyproline was found to be one of the main contributors to activity, as were the hydrophobic residues 5–7. Interestingly, the dihydroxyisoleucine at position 3 has been the source of some controversy (see below). Largely thought to be responsible for alimentary uptake and cell penetration, this unnatural amino acid can be substituted for Ile with minimal loss of activity in vitro but complete loss in vivo.[8] Despite a wealth of synthetic derivatives and corresponding IC_{50} values, the structural components necessary for this natural product to inhibit transcription continue to pique the curiosity of chemists and biologists alike, as it has for more than 70 years.[1]

To the benefit of synthetic efforts to understand the structure–activity relationships (SARs) of amanitin, several recent landmark papers have provided Ångstrom-level insight into the molecular basis of eukaryotic transcription initiation and elongation catalysed by the ten-subunit megadalton RNA polymerase II holoenzyme complex.[15–25] A natural consequence of these crystallographic studies was the identification of the amanitin binding site within the RNA pol II crystal, which confirmed early kinetic data suggesting the toxin binds to an allosteric site within a protein fold, not to the active site of RNA pol II.[17] The allosteric binding gives rise to a conformational change that leads to non-competitive inhibition of mRNA synthesis as well as a series of consequential dynamic cellular events, including the proteolysis of pol II and apoptotic cell death.[26–28]

In the post-proteomic era, the recognition of pol II by amanitin represents a natural and timely paradigm for inducing enzymatic inhibition; the desire to bind to a protein fold rather than mimicking the transition state. The co-crystal structure provided a static snapshot of some of the discrete hydrogen-bonding interactions revealing the basis for amanitin's extraordinary potency. Despite extensive in vitro SAR studies on various synthetic toxins, only one structure of the natural toxin bound to pol II has been obtained, and there are very few studies that provide ground-state structural analysis of the less toxic synthetic derivatives.[8,29,30] Co-crystal structures of synthetic derivatives with pol II remain undetermined and of potential interest for the elaboration of a complete SAR profile. For now, the basis for the toxicity of amanitin remains subtle and not entirely understood.

Given the controversy surrounding the role of the dihydroxyisoleucine at position 3, numerous derivatives have been prepared at this position.[9,12,13] Nevertheless, structural investigation of substitutions at position 3 has been limited to crystal structures of Ile^3-*S*-deoxo-amaninamide[29] and γ(*R*)-hydroxy-Ile^3-*S*-deoxo-amaninamide,[13] and detailed solution-structure analyses of L-Ala^3 and D-Ala^3 amatoxins.[31] These studies have raised questions as to the importance of the extent of oxidation at this position, the stereochemistry at C_α and the consequences of this on the overall structure. In the case of L-Ala^3 and D-Ala^3, solution structures were accompanied by circular dichroism data, in which at ≈230 nm an inverted Cotton effect was observed for the D-epimer. The intriguing possibility of "in–out" atropisomers (see Scheme 2) has been proposed to explain this inverted Cotton effect in previous reports on amatoxins.[12] However, ^{1}H NMR analysis showed the presence of a βI- and βII-turn for the L- and D-epimers, respectively, and it was suggested that this β-turn variation was responsible for the difference in CD spectra.

As we have been interested in amanitin as a synthetic ligand capable of recognising protein folds for use as a probe in cell biology, we have been investigating synthetic strategies to build libraries of amatoxins and further investigate the structural requirements for this exceptionally strong binding. Herein we report an improved synthetic strategy to access this family of bicyclic peptides, with the goal of eventually developing a library thereof. In so doing, we have validated our synthetic approach in the synthesis of the relatively non-toxic Pro^2-Ile^3-*S*-deoxo-amaninamide, utilising the more stable dipeptide precursor Tr-Hpi-Xaa-OH,[7] and a solid-phase peptide-synthesis strategy, with a view to higher yields and application in a library synthesis. Despite an improvement in synthetic applicability and ease, our synthetic efforts resulted in the isolation of two unique products, both with the desired mass but with an inverted Cotton effect at 230 nm in the CD spectra. This raised questions as to the conformational and stereochemical identity of both products. Notably, these two products were reproducibly obtained over the course of several independent syntheses in our laboratory, despite the fact that in past syntheses of amatoxins there have been few reports of multiple products being formed. Thorough characterisation of these two products, including the first crystal structures of Pro^2-D-*allo*-Ile^3-*S*-deoxo-amaninamide, are reported, concluding that epimerisation at position 3 results in the formation of a βII-turn in ring I. In addition, we observe two distinct conformations of this synthetic toxin (in ring II) within the same crystal. The implications for toxicity and bioactivity are briefly discussed.

Results and Discussion

For the purposes of this study we decided to use readily available L-amino acids (and not their hydroxylated congeners) in the pursuit of the synthetic amatoxin, Pro^2-Ile^3-*S*-deoxo-amaninamide (**1**). A simple consideration of the retrosynthesis of this peptide suggested a resin-bound linear peptide of the sequence Tr-Hpi-Gly-Ile-Gly-Cys(Tr)-Asn(Tr)-Pro-Ile-resin would be a suitable precursor. This would allow the use of standard Fmoc solid-phase peptide-synthesis strategies and a Tr-Hpi-Gly-OH dipeptide.[#][7] Solid-phase chemistry was performed on a 2-chlorotrityl resin with Fmoc-protected amino acids using 2-(1*H*-benzatriazole-1-yl)-1,1,3,3-tetramethyluronium hexafluorophos-

[#] At this point we had not considered other possible routes such as using an Hpi internally within the peptide backbone.

phate/*N,N*-diisopropylethylamine (HBTU/DIPEA) coupling steps and 20% piperidine deprotective steps, to construct the hexapeptide **2** (Scheme 1). The Tr-Hpi-Gly-OH dipeptide was synthesised as we described previously[7] and this was coupled to the resin-bound hexapeptide in a similar fashion. Following extensive washing, the linear octapeptide (**3**) was treated with trifluoroacetic acid (TFA) to simultaneously cleave the peptide from the resin, remove all trityl protecting groups and transform the Hpi moiety to a tryptathionine cross-link by means of the Savige–Fontana reaction. The crude product was initially purified by using a Sep Pak C-18 column to give a white solid residue and this was further purified by reverse-phase HPLC (see the Experimental Section for details). Pure monocyclic product (**4**) possessed a strong UV absorption at 290 nm, characteristic ^{1}H NMR chemical shifts and gave the expected HRMS parent ion. The final backbone coupling was achieved by using (benzotriazol-1-yloxy)-tripyrrolidino-phosphonium hexafluorophosphate/1-hydroxybenzotriazole (PyBOP/HOBt) at high peptide dilution (1 mM) to minimise any dimeric products forming. The crude product was initially purified on silica gel ($CHCl_3$/MeOH/H_2O 90:13:1) affording a product with the characteristic UV absorbance and the expected HRMS. However, on further purification by HPLC two products were isolated (denoted **1a** and **1b**). These could not be resolved by silica gel column or thin layer chromatography ($CHCl_3$/MeOH/H_2O 90:13:1).

MS/MS provided further confirmation of the correct structures in both cases, with nearly identical fragmentation patterns for the pair of compounds (data not shown). However, comparison of the NMR spectra of the respective compounds **1a** and **1b** showed a few distinct differences. The differences between **1a** and **1b** are further underscored in the CD spectra (Figure 2); compound **1b** displayed a large negative Cotton effect at 230 nm, whereas compound **1a** had a positive value in this region. Comparison of these CD spectra with spectra for compounds in the literature allowed us to identify **1b** as the desired product, Pro^2-Ile^3-*S*-deoxo-amaninamide,[9,33] however, the exact conformational and stereochemical identity of **1a** remained unknown.

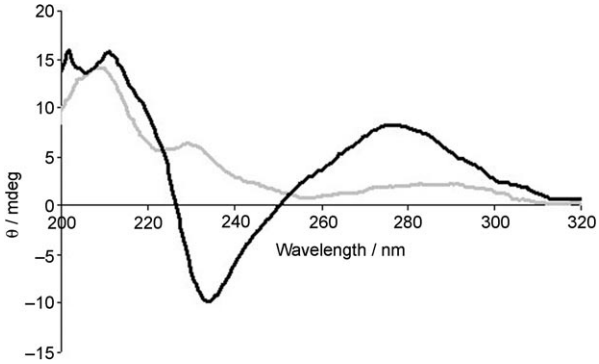

Figure 2. CD spectra for the amatoxin derivatives **1a** (——) and **1b** (——).

We sought to fully characterise these products not only to improve the synthetic methods reported herein, but to better understand how structural variations of synthetic amanitins contribute to in vitro activity. This was particularly important in light of the unresolved question as to the inverted Cotton effect in the CD and its relationship to structure. Because these compounds could not be interconverted, the possibility of *cis–trans* isomers of proline was excluded (see Supporting Information). It occurred to us that these two isomers could be one of two different possible types: 1) epimers of the C-terminal Ile formed during the final coupling step; 2) "in–out" atropisomers that arose during closing of the second ring, whereby formation of the two atropisomers would depend on which side of the pre-formed ring the C-terminal carbonyl group of Ile approached the amine of Trp (Scheme 2). Provided that the tryptathionine bridge could not invert through the polyamide ring, two atropisomers would be formed, the possibility of which has been discussed previously by Zanotti et al., albeit without concrete experimental evidence.[12,31,32]

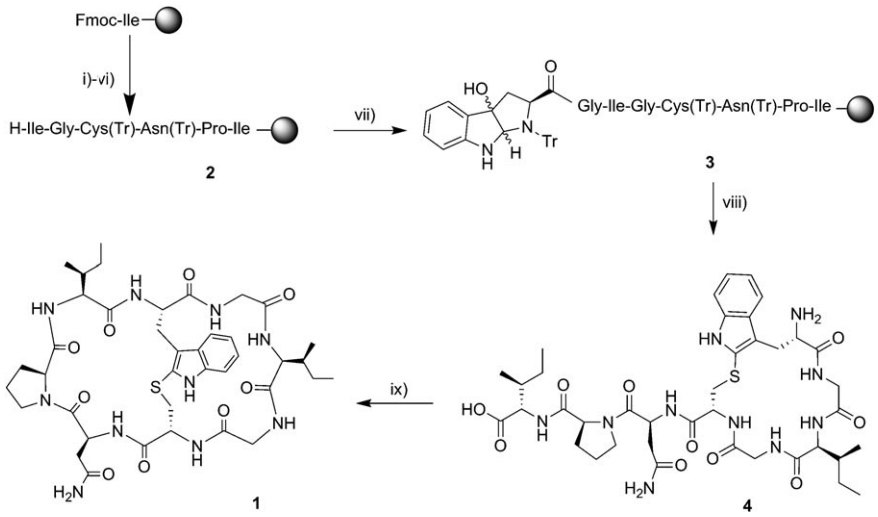

Scheme 1. Synthesis of Pro^2-Ile^3-*S*-deoxo-amaninamide **1**. For the solid-phase synthesis i)–v) deprotection (piperidine/DMF (20%), RT, 10 min) and coupling (Fmoc-Xaa-OH (4 equiv), HBTU (4 equiv), DIPEA (0.5%), DMF, RT, 20 min) steps were repeated with each amino acid, for which Xaa = i) Pro, ii) Asn(Tr), iii) Cys(Tr), iv) Gly, v) Ile; vi) piperidine/DMF (20%), RT, 10 min; vii) Tr-Hpi-Gly-OH (3 equiv), HBTU (3 equiv), DIPEA (0.5%), DMF, RT, 1 h; viii) TFA, RT, 5 h; ix) PyBOP (3 equiv), HOBt (3 equiv), DIPEA (5 equiv), DMF, RT, 18 h.

The CD spectra of compounds **1a** and **1b** could be

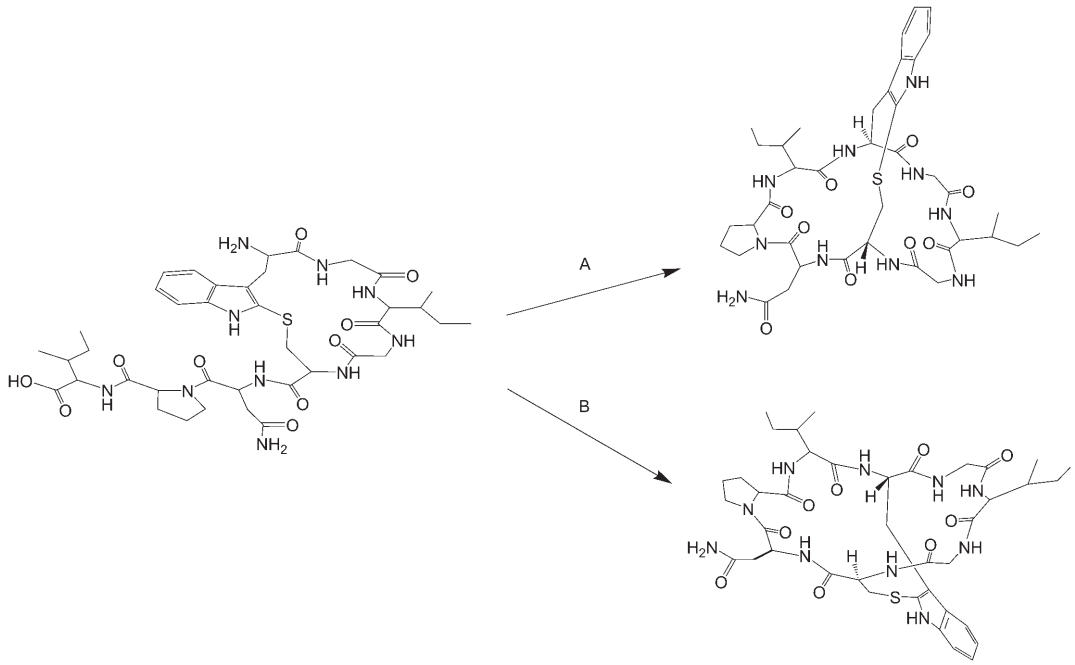

Scheme 2. Hypothetical formation of two atropisomers during the final coupling step. The C terminus can approach the N terminus from either below the plane (A) or above the plane (B) of the preformed ring.

consistent with the formation of atropisomers or very different topological conformations, based on prior reports; a positive Cotton effect between 220 and 240 nm has been reported as an atropisomeric or "iso" structure, whereas a negative Cotton effect (cf. α-amanitin) has been suggested to be the "natural" atropisomer. If this were indeed the case, we can assign **1a** as the "iso" structure and **1b** as the "natural" isomer. In contrast to an "in–out" topological difference in conformation, two different β-turn structures may also explain the inverted variations in the CD spectra (220–240 nm). These two types of β-turns were observed following deliberate incorporation of either an L- or D-alanine at position 3 in synthetic amatoxins.[31] In our case, we entertained the possibility of epimerisation in the final coupling step (with a C-terminal Ile) to give two epimers (position 3: L-Ile or D-*allo*-Ile), one of which possesses a βI-turn and the other a βII-turn. Alternatively, epimerisation at position 3 might have resulted in not only a different β-turn, but also a significantly different global shape of the toxin reminiscent of "in–out" atropisomers. Thus, substantiation of epimerisation and full characterisation of the conformational effects of an epimer at position 3 (i.e., D-*allo*-Ile) with regard to both structure and activity became the focus of this study.

Confirmation was obtained when a crystal of compound **1a** was grown ($MeOH/H_2O$ 5%). X-ray diffraction data obtained were sufficient to generate a fully integrated peptide structure (Figure 3) in the presence of several methanol molecules within the unit cell (see Supporting Information), which contained two molecules of **1a**. Both of these molecules of **1a** have an epimerised centre at C_α of Ile[3], that is, D-*allo*-Ile and not the original L-Ile. In addition, the β-turn in this portion of the peptide is characteristic of a βII-turn, in agreement with the NOE data we collected (see Supporting Information) and a previous report based on ^{1}H NMR studies with D-Ala at this position.[31] Never before has a

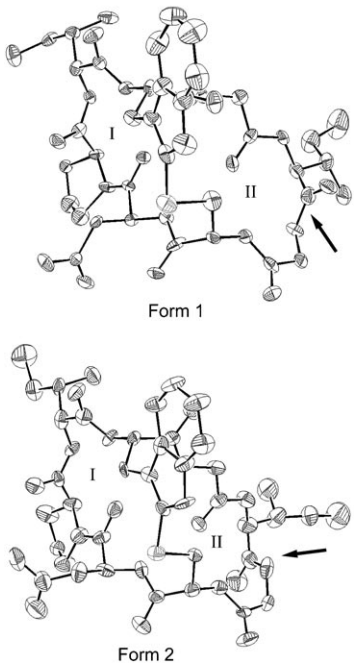

Figure 3. Two conformations of compound **1a** in the crystalline state (forms 1 and 2), displaying the D-*allo*-Ile at position 3. The same βII-turn (residues 1–4) is shown in ring I in both structures. A βII-turn is found in ring II in form 1 and a βI-turn is found in ring II in form 2. Note: This is not a unit cell, but a picture showing the two crystallised forms for comparison.

crystal structure of an amatoxin been obtained to confirm the presence of this βI-turn at an epimerised centre. This work thus sheds a new light on some of the early work on epimeric Ala[3] derivatives that displayed similar CD spectra.[12]

The two conformations of **1a** in the crystal unit cell are almost identical in structure except for a variation in the orientation of the amide bond between the residues Ile[6] and Gly[7] in ring II (Figure 3). In one structure the carbonyl of the amide bond is oriented to the same side as the tryptathionine (βII-turn), whereas the other structure shows it inverted (βI-turn). This is quite apparent when forms 1 and 2 are overlayed (Figure 4). Interestingly, flipping of this β-turn has not been observed in any of the other crystal or NMR structures of amatoxin derivatives, and until now it has been assumed that this part of the ring was very rigidly held in a βII-turn structure, which is crucial for amatoxin binding.[33] It is impossible to say whether this variation in turn structure of residues 5–8 is indicative of a less rigid structure than previously thought, or a crystallisation artifact. One aspect worth noting is that it seems both structures maintain the Ile[6] side chain in approximately the same area of space, which is thought to be vital for binding a hydrophobic pocket of RNA pol II.[33]

To investigate the extent to which this epimerisation changes the global amatoxin structure, we compared the structure of **1a** with that of a previously crystallised amanitin. The structure of β-amanitin (identical to α-amanitin except for an Asp at position 1) was used, because it represents the most biologically potent amatoxin crystallised to date.[34,35] The comparison was made between form 1 of **1a** with a βII-turn through residues 5–8, because this resembled the βII-turn in amanitin. To highlight some of the differences between **1a** and α-amanitin, both structures were overlayed by holding the indole ring fixed in both structures (Figure 5). The relative angles of the tryptathionine linkage to the peptide backbone are shown to vary by about 10° between the two structures. This could explain the smaller Cotton effect between 280–310 nm in the CD spectra for **1a**, relative to other amatoxins. Apart from this variation in angle, ring II formed by Trp[4]-Gly[5]-Ile[6]-Gly[7]-Cys[8] is very similar in both structures. Ring I containing Cys[8]-Asn[1]-Pro[2]-D-*allo*-Ile[3]-Trp[4] displays a few differences relative to the equivalent ring in β-amanitin, but this also happens to contain three different

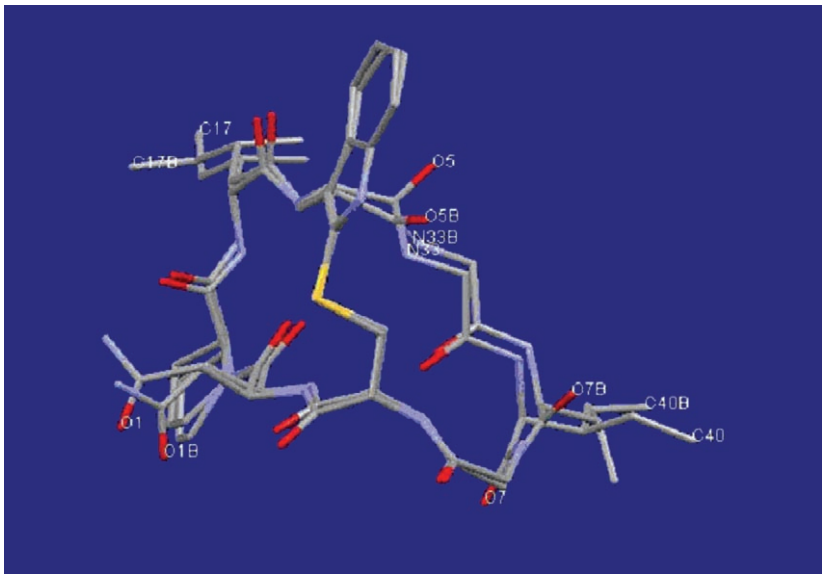

Figure 4. An overlay of the two conformations of the crystal structure of compound **1a**. The two tryptathionine linkages have been superimposed; note the difference in orientation of the amide carbonyl of Ile[6].

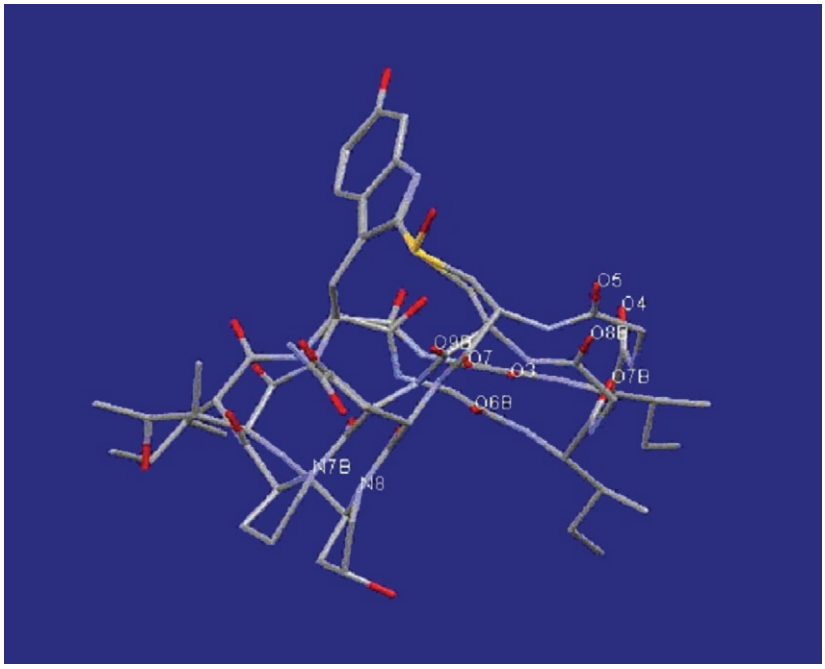

Figure 5. An overlay of the crystal structure of compound **1a** and the previously crystallised β-amanitin,[34,35] in which the two tryptathionine linkages have been superimposed.

residues (Asp[1]-Hyp[2]-Dhi[3]), which makes it difficult to specify exactly what is responsible for the observed variations in global structure.

Despite the presence of these different functionalities, the two structures share many overall structural and conformational similarities. Of note is the observation that epimerisation of C_α at position 3 has little effect on the global structure found by X-ray diffraction in the crystalline form. Additionally, in both cases it appears that the side chain of position 1 (Asn or Asp) is not involved in an intramolecular hydrogen bond to stabilise the β-turn structure, contrary to reports for some other amatoxin structures (βII-turns).[8,29]

Having realised the structural nature of these epimers, we tested compounds **1a** and **1b** in an in vitro cell-based bioactivity assay, using hepatocytes (Figure 6). This study indicated low levels of inhibition for both compounds **1a** and **1b** ($\approx 10^3$ less toxic than α-amanitin). Tentatively, **1b** appears slightly more toxic than **1a**, and these values are in the same order as for the D- and L-Ala[3]-*S*-deoxo-amaninamide analogues studied previously.[31] This suggests that the stereochemical conformation of C_α of Ile[3] is not of high importance for toxicity, which is in good agreement with reports of this position being disordered in the crystal structure of α-amanitin with yeast RNA pol II.[17] It is nonetheless recognised that at these low levels of toxicity relative to that of α-amanitin, the differences in toxicity may be ascribed to other phenomena, such as issues of cell permeability.

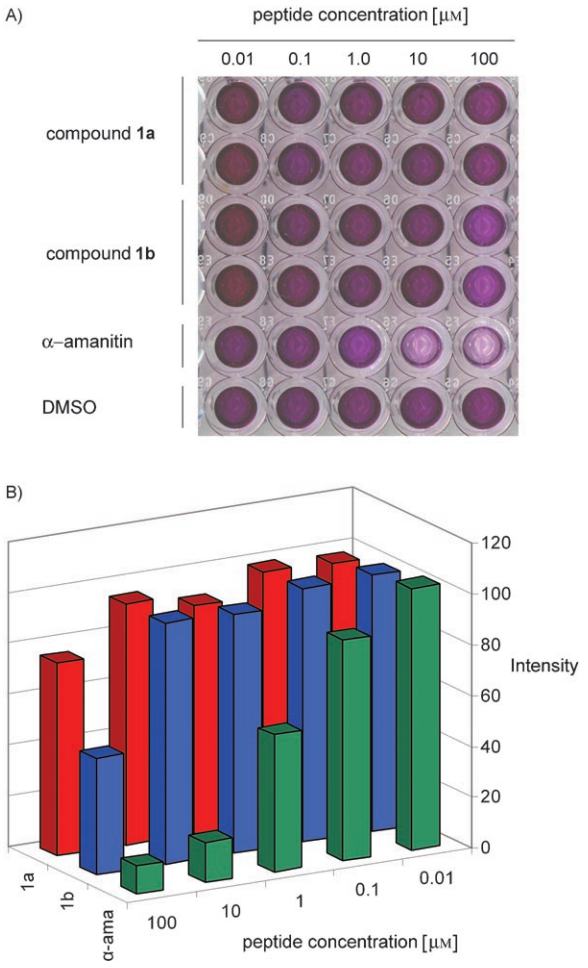

Figure 6. Cell-toxicity assay using HepG2 cells with an MTT-based readout (dye is reduced and causes an intense purple colour in healthy cells). Compound **1a**, **1b** and the standard reference of α-amanitin were studied at five concentrations (100, 10, 1.0, 0.1, 0.01 μM). A) Plate showing relative intensity of purple dye; B) bar chart representing average intensity values.

Conclusion

Despite previous reports on various amanitin syntheses in which epimers at position 3 had not been observed or reported, in our hands, the final macrocyclisation step using PyBOP is accompanied by a surprisingly significant amount of epimerised product. Nevertheless, the identification of two products with an inverted Cotton effect relates to an unanswered question as to the exact nature of the structural attributes of these products. Indeed some of these previous studies involved substitutions of D-amino acids at position 3, which gave rise to toxins with inverted CD spectra, as we have seen in our work. The crystal structure we provide here strongly discounts the possibility of "in–out" atropisomers and instead demonstrates that the inverted Cotton effect is simply due to a difference in the β-turn structure. Consequently, we conclude that **1a** has a βI-turn, in contrast to the natural product, whereas **1b** retains the βII-turn characteristic of the natural product. Furthermore, this work also allows us to relate the effect of stereochemistry at C_α of position 3 with the relative in vitro activity of each conformation.

For the first time, evidence of some variation in turn structure between residues 5 and 8 in the crystalline state of an amatoxin is reported. The basis for observing two β-turns within the same crystal in ring II remains puzzling. This could be simply an artifact of crystallisation, and in solution form 1 may predominate or rapidly interconvert on the NMR timescale. If both conformations are rapidly interconverting, this would suggest that the amatoxin is either able to adopt the best fit to the enzyme, or that there is a degree of conformational flexibility in pol II at Gln767, Arg726 and Val719, such that both conformations can be accommodated in the active site.[17] Although the amatoxin investigated can clearly form two β-turns in the crystalline state, neither the X-ray crystal presented herein, nor a future NMR solution structure would necessarily represent the conformation responsible for enzyme-bound inhibition. Although an NMR solution structure would nicely complement this work, we opted for X-ray crystal-structure analysis to definitively identify the stereochemistry at C_α and thereby state unambiguously that the conformations borne out in the solution-phase CD spectra are the result of epimers and not atropisomers.

Having substantiated that this synthetic route gives two epimers, it will be interesting to correlate the structural differences of epimers at position 3 bearing hydroxyproline

and its analogues at position 2. Such compounds are currently being prepared and their SARs will be reported in the near future. With regards to future syntheses of amanitin, one must consider other coupling agents that are better designed to avoid racemisation, or otherwise deliberately introduce a D-amino acid at position 3 with an eye to using this approach to enhancing the macrocyclisation yield.[36–39] Nevertheless, this strategy is suitable for further development into a combinatorial approach to generate a library of related structures that have great potential to inhibit various target RNA polymerases, as well as binding other unrelated protein folds.

Finally, it seems the bicyclic structure can be viewed as a fairly rigid scaffold that could be decorated with side chains capable of hydrogen bonding or fitting hydrophobic pockets. Synthesis of a library of amanitin-like bicyclic peptides should reveal a great deal of information on the nature of this binding interaction, and perhaps it could even lead to molecules with greater binding strength than the natural analogues, or identification of new amatoxins with specificity for bacterial RNA polymerases.

Experimental Section

Monocyclic H-Trp-Gly-Ile-Gly-Cys-Asn-Pro-Ile-OH (4)

Solid-phase peptide synthesis of 2,3: 2-Chlorotrityl resin functionalised with Fmoc-Ile-OH (0.25 g, resin loading: 1.1 mmol g^{-1}) was used. Deprotection steps were with piperidine (20%) in DMF for 10 min. Coupling was preformed with Fmoc-AA-OH (4 equiv), HBTU (4 equiv), DIPEA (0.5%) agitating for 20 min with all standard amino acids to generate the linear hexapeptide **2**. Coupling of Tr-Hpi-Gly-OH (0.5 g, 3 equiv) was with HBTU (0.3 g, 3 equiv), DIPEA (0.5%) with shaking for 1 h. The resin was washed extensively with DMF (×10) and CH_2Cl_2 (×5) to yield resin-bound octapeptide (**3**). A small sample was taken and treated with hexafluoroisopropanol (HFIP) to cleave the compound from the resin, and checked by mass spectrometry (see Supporting Information). TFA (10 mL) was added to **3** and stirred for 5 h at RT. Solvent was evaporated in vacuo and redissolved in water before evaporating again. This was repeated three times. The residue was dissolved in MeOH, and filtered to remove resin. The filtrate was concentrated, and then diluted with H_2O for purification on a C18 SepPak column, eluting with H_2O/MeOH (0–100%). Fractions were collected and studied by TLC (BuOH/AcOH/H_2O 4:1:1) and UV spectroscopy. Those fractions containing the characteristic tryptathionine UV were combined and evaporated to dryness. The residue was then purified by HPLC (buffer A = H_2O + 0.01 % TFA; buffer B = MeCN + 0.05 % TFA). Pure product was combined to yield a white solid residue of monocyclic octapeptide **4** (15 mg, 7%). R_f=0.4 (*n*BuOH/AcOH/water 4:1:1); ^{1}H NMR (600 MHz, [D$_6$]DMSO): δ=12.55–12.45 (brs, 1H; COOH), 11.43 (s, 1H; NH^{indole}), 9.07 (s, 1H; $NHCO^{Gly}$), 8.27 (d, J=8.5 Hz, 1H; $NHCO^{Cys}$), 8.23 (d, J=8.2 Hz, 1H; $NHCO^{Ile}$), 8.20 (d, J=7.7 Hz, 1H; $NHCO^{Asn}$), 7.96 (brs, 2H; $CONH_2^{Asn}$), 7.91 (d, J=8.7 Hz, 1H; $NHCO^{Ile}$), 7.87–7.81 (d, J=7.6 Hz, 1H; ArH^6), 7.37–7.32 (m, 2H; ArH^4, $NHCO^{Gly}$), 7.16 (t, J=7.6 Hz, 1H; ArH^5), 7.05 (t, J=7.6 Hz, 1H; ArH^7), 4.72 (q, J=13.7, 6.5 Hz, 1H; $CH^{Asn\alpha}$), 4.36 (t, J=7.8 Hz, 1H; $CH^{Trp\alpha}$), 4.12 (br, 1H; $CH^{Ile\alpha}$), 4.07 (t, J=7.3 Hz, 1H; $CH^{Cys\alpha}$), 4.04–4.00 (m, 1H; $CH^{Ile\alpha}$), 3.98 (t, J=8.9 Hz, 1H; $CH^{Pro\alpha}$), 3.93 (dd, J=12.0, 5.0 Hz, 1H; $CH^{Gly\alpha}$), 3.83 (dd, J=15.4, 4.9 Hz, 1H; $CH^{Gly\alpha}$), 3.77 (dd, J=15.8, 5.4 Hz, 1H; $CH^{Gly\alpha}$), 3.69 (dd, J=16.8, 3.6 Hz, 1H; $CH^{Gly\alpha}$), 3.64–3.44 (m, 4H; $CH_2^{Pro\delta}$, $CH^{Pro\beta,Cys\beta}$), 2.83 (dd, J=14.9, 4.3 Hz, 1H; $CH^{Pro\beta}$), 2.75 (t, J=12.3 Hz, 1H; $CH^{Cys\beta}$), 2.70–2.62 (m, 1H; $CH^{Asn\beta}$), 2.36 (dd, J=15.8, 6.9 Hz, 1H; $CH^{Asn\beta}$), 2.00–1.70 (m, 6H; $CH_2^{Pro\gamma,Trp\beta,Ile\beta}$), 1.51–1.05 (m, 4H; $CH_2^{Ile\gamma}$), 0.88–0.76 ppm (m, 12H; $CH_3^{Ile\gamma',Ile\delta}$); ^{13}C NMR (150 MHz, [D$_6$]DMSO): δ=172.9 ($CONH_2^{Asn}$), 171.4 (COOH), 171.3 (CO^{Asn}), 171.2 (CO^{Pro}), 169.9 (CO^{Trp}), 169.5 (CO^{Ile}), 169.4 (CO^{Cys}), 168.8 (CO^{Gly}), 168.4 (CO^{Gly}), 137.4 (C^{7a}), 126.7 (C^{3a}), 126.5 (C^2), 122.3 (CH^5), 119.1 (CH^4), 118.7 (CH^6), 113.5 (C^3), 111.2 (CH^7), 59.2 ($CH^{Trp\alpha}$), 59.1 ($CH^{Pro\alpha}$), 56.3 ($CH^{Cys\alpha}$), 52.5 ($CH^{Ile\alpha}$), 51.1 ($CH^{Ile\alpha}$), 47.9 ($CH^{Asn\alpha}$), 46.7 ($CH_2^{Pro\delta}$), 43.5 ($CH_2^{Gly\alpha}$), 42.7 ($CH_2^{Gly\alpha}$), 37.4 ($CH_2^{Cys\beta}$), 36.7 ($CH_2^{Asn\beta}$), 36.1 ($CH^{Ile\beta}$), 35.4 ($CH^{Ile\beta}$), 28.9 ($CH_2^{Trp\beta}$), 27.7 ($CH_2^{Pro\beta}$), 24.7 ($CH_2^{Ile\gamma}$), 24.6 ($CH_2^{Ile\gamma}$), 24.2 ($CH_2^{Ile\gamma}$), 15.6 ($CH_3^{Ile\gamma'}$), 15.4 ($CH_3^{Ile\gamma'}$), 11.3 ($CH_3^{Ile\delta}$), 10.7 ppm ($CH_3^{Ile\delta}$); ES$^+$/MS: m/z: 857.4 $[M+H]^+$, 879.5 $[M+Na]^+$; HRMS (ESI): m/z: calcd for $C_{39}H_{57}N_{10}O_{10}S$: 857.3980 $[M+H]^+$; found: 857.3987.

Bicyclic amatoxins 1a and 1b: Compound **4** (15 mg, 0.018 mmol) was dissolved in dry DMF (15 mL) under an atmosphere of nitrogen. PyBOP (27 mg, 0.052 mmol), HOBt (8 mg, 0.053 mmol) and DIPEA (18 μL, 0.10 mmol) were added. The mixture was stirred for 18 h at RT. Solvent was removed in vacuo and the mixture was initially purified by silica gel column chromatography ($CHCl_3$/MeOH/H_2O 90:13:1). Pure fractions were combined to yield crude product as a white solid. This solid was dissolved in MeOH/H_2O and further purified by HPLC (buffer A = H_2O + 0.01% TFA; buffer B = MeCN + 0.05% TFA); two peaks were collected, which were denoted **1a** (3.0 mg (20%), faster to elute) and **1b** (1.6 mg (11%), slower to elute). R_f=0.5 ($CHCl_3$/MeOH/water 90:13:1).

Pro^2-D-*allo*-Ile^3-*S*-deoxo-amaninamide (1a): ^{1}H NMR (600 MHz, [D$_6$]DMSO): δ=11.24 (s, 1H; NH^{indole}), 8.83 (t, J=6.0 Hz, 1H; $CONH^{Gly}$), 8.55 (d, J=5.2 Hz, 1H; $CONH^{Ile}$), 8.44 (d, J=9.7 Hz, 1H; $CONH^{Ile}$), 8.16–8.14 (m, 2H; $CONH^{Asn,Trp}$), 7.69 (brs, 1H; $CONH^{Gly}$), 7.54–7.50 (m, 2H; CH^{indole}, $CONH^{Cys}$), 7.28–7.23 (m, 2H; CH^{indole}, NH^{Asn}), 7.12 (t, J=7.5 Hz, 1H; CH^{indole}), 7.02 (t, J=7.5 Hz, 1H; CH^{indole}), 6.89 (brs, 1H; NH^{Asn}), 4.95–4.82 (m, 2H; $CH^{Trp\alpha,Asn\alpha}$), 4.62–4.56 (m, 2H; $CH^{Cys\alpha,Pro\alpha}$), 4.43 (dd, J=6.1, 3.2 Hz, 1H; $CH^{Ile\alpha}$), 3.95 (dd, J=12.4, 5.6 Hz, 1H; $CH^{Gly\alpha}$), 3.90 (dd, J=10.5, 7.0 Hz, 1H; $CH^{Gly\alpha}$), 3.80–3.70 (m, 3H $CH^{Ile\alpha,Pro\delta,Trp\beta}$), 3.64–3.51 (m, 3H; $CH^{Gly\alpha,Pro\delta}$), 3.40–3.30 (m, 1H; $CH^{Cys\beta}$), 3.01 (d, J=10.8 Hz, 1H; $CH^{Cys\beta}$), 2.79 (dd, J=9.5, 4.7 Hz, 1H; $CH^{Trp\beta}$), 2.68 (dd, J=8.8, 7.2 Hz, 1H; $CH^{Asn\beta}$), 2.55–2.45 (m, 1H; $CH^{Asn\beta}$), 2.21–2.13 (m, 2H; $CH^{Pro\beta,Ile\beta}$), 2.12–2.06 (m, 1H; $CH^{Ile\gamma}$), 1.96–1.88 (m, 1H; $CH^{Ile\gamma}$), 1.83–1.75 (m, 1H; $CH^{Pro\beta}$), 1.70–1.62 (m, 1H; $CH^{Ile\beta}$), 1.60–1.54 (m, 1H; $CH^{Ile\gamma}$), 1.26–1.10 (m, 3H; $CH^{Ile\gamma}$, $CH_2^{Pro\gamma}$), 0.86–0.78 ppm (m, 12H; $CH_3^{Ile\gamma,Ile\delta}$); ^{13}C NMR (150 MHz, [D$_6$]DMSO): δ=173.1 ($CONH_2^{Asn}$), 171.9 (CO^{Asn}), 170.6 (CO^{Pro}), 170.3 (CO^{Trp}), 169.9 (CO^{Ile}), 169.6 (CO^{Ile}), 169.5 (CO^{Cys}), 168.4 (CO^{Gly}), 167.7 (CO^{Gly}), 136.8 (Trp C^{7a}), 127.2 (C^{3a}), 125.4 (C^2), 122.3 (CH^5), 118.8 (CH^6), 118.7 (CH^4), 115.5 (C^3), 111.1 (CH^7), 60.2 ($CH^{Pro\alpha}$), 59.1 ($CH^{Ile\alpha}$), 55.1 ($CH^{Ile\alpha}$), 54.1 ($CH^{Trp\alpha}$), 51.8 ($CH^{Cys\alpha}$), 49.4 ($CH^{Asn\alpha}$), 47.3 ($CH_2^{Pro\delta}$), 42.1 (2$CH_2^{Gly\alpha}$), 37.6 ($CH_2^{Cys\beta}$), 36.8 ($CH_2^{Asn\beta}$), 34.3 ($CH^{Ile\beta}$), 34.2 ($CH^{Ile\beta}$), 28.5 ($CH_2^{Pro\beta}$, $CH_2^{Trp\beta}$), 26.0 ($CH_2^{Pro\gamma}$), 25.3 ($CH_2^{Ile\gamma}$), 24.9 ($CH_2^{Ile\gamma}$), 15.1 ($CH_3^{Ile\gamma'}$), 14.6 ($CH_3^{Ile\gamma'}$), 11.6 ($CH_3^{Ile\delta}$), 10.5 ppm ($CH_3^{Ile\delta}$); ES$^+$/MS: m/z: 838.4 $[M+H]^+$, 861.5 $[M+Na]^+$; HRMS (ESI): m/z: calcd for $C_{39}H_{54}N_{10}O_9SNa$: 861.3694 $[M+Na]^+$; found: 861.3681.

Pro^2-Ile^3-*S*-deoxo-amaninamide (1b): R_f=0.5 ($CHCl_3$/MeOH/water 90:13:1); ^{1}H NMR (500 MHz, [D$_6$]DMSO): δ=11.21 (brs, 1H; NH^{indole}), 8.80 (t, J=6.2 Hz, 1H; $CONH^{Gly}$), 8.48 (s, 1H; $CONH^{Asn}$), 8.43 (d, J=3.8 Hz, 1H; $CONH^{Ile}$), 8.22 (s, 1H; NH^{Asn}), 8.08–8.00 (m, 4H; $NH^{Gly,Ile,Trp,Cys}$), 7.58 (d, J=7.5 Hz, 1H; ArH^{indole}), 7.49 (s, 1H; NH^{Asn}), 7.23 (d, J=7.5 Hz, 1H; ArH^{indole}), 7.09 (t, J=7.5 Hz, 1H; ArH^{indole}), 6.99 (t, J=7.5 Hz, 1H; ArH^{indole}), 4.88 (m, 1H; $CH^{Trp\alpha}$), 4.75 (d, J=3.2 Hz, 1H; $CH^{Asn\alpha}$), 4.54 (m, 1H; $CH^{Cys\alpha}$), 4.28 (dd, J=18.5, 8.8 Hz, 1H; $CH^{Gly\alpha}$), 4.19–4.12 (m, 2H; $CH^{Pro\alpha,Ile\alpha}$), 3.94 (t, J=8.3 Hz, 1H; $CH^{Pro\delta}$), 3.85 (dd, J=16.9, 6.9 Hz, 1H; $CH^{Gly\alpha}$), 3.65–3.58 (m, 2H; $CH^{Pro\delta,Ile\alpha}$), 3.45–3.39 (m, 1H; $CH^{Gly\alpha}$), 3.38–3.31 (m, 1H; $CH^{Asn\beta}$), 3.36–3.28 (m, 1H; $CH^{Gly\alpha}$), 3.23 (t, J=13.9 Hz, 1H; $CH^{Trp\beta}$), 3.09–3.04 (m, 1H; $CH^{Trp\beta}$), 3.03–2.98 (m, 2H; $CH^{Asn\beta,Cys\beta}$), 2.72 (dd, J=9.6, 8.5 Hz, 1H; $CH^{Cys\beta}$), 2.35–2.30 (m, 1H; $CH^{Pro\beta}$), 2.01–1.97 (m, 1H; $CH^{Pro\gamma}$), 1.96–1.89 (m, 1H; $CH^{Ile\beta}$), 1.86–1.79 (m, 1H; $CH^{Pro\gamma}$), 1.72–1.65 (m, 1H; $CH^{Pro\beta}$), 1.55–1.05 (m, 5H; $CH_2^{Ile\gamma}$, $CH^{Ile\beta}$), 0.88 (d, J=6.8 Hz, 3H; $CH_3^{Ile\gamma}$), 0.85–0.75 ppm (m, 9H; $CH_3^{Ile\gamma,Ile\delta}$); ^{13}C NMR (75 MHz, [D$_6$]DMSO): δ=174.5 ($CONH_2^{Asn}$), 173.7(CO^{Asn}), 172.7 (CO^{Pro}), 172.3 (CO^{Trp}), 172.3 (CO^{Ile}), 171.8 (CO^{Ile}), 171.8 (CO^{Cys}), 170.1 (CO^{Gly}), 169.5 (CO^{Gly}), 138.4 (C^{7a}), 128.9 (C^{3a}), 126.4 (C^2), 124.1 (CH^5), 122.3 (CH^4), 120.5 (CH^6), 117.8 (C^3), 113.0

(CH^{7}), 65.3 ($CH^{Trp\alpha}$), 61.0 ($CH^{Pro\alpha}$), 59.8 ($CH^{Ile\alpha}$), 55.4 ($CH^{Cys\alpha}$), 54.6 ($CH^{Ile\alpha}$), 52.6 ($CH^{Asn\alpha}$), 44.3 ($CH_2^{Pro\delta}$), 41.4 ($2CH_2^{Gly\alpha}$), 37.5 ($CH_2^{Cys\beta}$), 36.4 ($CH_2^{Asn\beta}$), 35.7 ($2CH^{Ile\beta}$), 31.8 ($CH_2^{Trp\beta}$), 27.1 ($CH_2^{Pro\beta}$), 26.9 ($2CH_2^{Ile\gamma}$), 17.7 ($CH_2^{Pro\gamma}$), 16.7 ($2CH_3^{Ile\gamma'}$), 12.5 ppm ($2CH_3^{Ile\delta}$); ES^+/MS: m/z: 838.4 $[M+H]^+$, 861.5 $[M+Na]^+$; HRMS (ES^+): m/z: calcd for $C_{39}H_{54}N_{10}O_9SNa$: 861.3696 $[M+Na]^+$; found: 861.3694.

Bioactivity assay: The relative toxicity of compounds **1a** and **1b** relative to the natural product α-amanitin was calculated by means of an MTT-based cytotoxicity assay. The assay is based on the principle that only live cells reduce yellow MTT (3-(4,5-dimethylthiazolyl-2)-2,5-diphenyltetrazolium bromide) to the purple formazan product. The human liver cancer cell line HepG2 (kind gift from Dr. D. Chen, UBC Chemistry) was grown at 37 °C and CO_2 (5 %) in minimal essential medium (MEM) α-medium (Invitrogen). For the MTT assay HepG2 cells were suspended in fresh medium (1×10^5 cells mL^{-1}) and 200 μL aliquots were made to a 96-well plate format. Cells in exponential phase of growth (incubated overnight at 37 °C in air containing 5 % CO_2) were exposed to the test compounds. All compounds were dissolved in dimethyl sulfoxide (DMSO) and serially diluted to create a range of concentrations from 100–0.01 μM final concentration (medium/DMSO 0.5 %). Control lanes with 1) DMSO and medium only and 2) DMSO, medium and HepG2 were included. The plate was incubated at 37 °C in air with CO_2 (5 %) for 72 h. Measurement of cell viability was done as follows: MTT (50 μL of a 2.5 mg mL^{-1} solution in phosphate-buffered saline) was then added to each well and the plate was incubated for a further 3 h. The contents of each well were then carefully aspirated off and DMSO (150 μL per well) was added to each well to dissolve the tetrazolium salts. The absorbances of each well were then studied at 570 nm by using a Beckman-Coulter DTX-800 plate reader. Average values of duplicate readings were made and normalised relative to the blank medium.

CCDC 658247 contains the supplementary crystallographic data for this paper. These data can be obtained free of charge from The Cambridge Crystallographic Data Centre via www.ccdc.cam.ac.uk/data_request/cif.

Acknowledgements

J.P.M. received a post-doctoral fellowship from The Royal Society, UK; D.M.P. received a Junior Career Award from the Michael Smith Foundation for Health Research in B.C.; this work was supported by U.B.C. start-up funds, funding from the Michael Smith Foundation for Health Research in B.C. and funding from the Canadian Institutes of Health Research. The CD spectrometer was provided through a grant from the Canada Foundation for Innovation to the Laboratory for Molecular Biophysics to Dr. Fred Rosell. Dr. Elena Polishchuk and Jessie Chen are gratefully acknowledged for their assistance with the toxicity assay, and Dr. Nick Burlinson for his help running NOE and 600 MHz NMR experiments.

[1] T. Wieland, H. Faulstich, *Experientia* **1991**, *47*, 1186–1193.
[2] G. Zanotti, C. Mohringer, T. Wieland, *Int. J. Pept. Protein Res.* **1987**, *30*, 450–459.
[3] G. Zanotti, T. Wieland, G. Dauria, L. Paolillo, E. Trivellone, *Int. J. Pept. Protein Res.* **1990**, *35*, 263–270.
[4] W. E. Savige, *Aust. J. Chem.* **1975**, *28*, 2275–2287.
[5] W. E. Savige, A. Fontana, *J. Chem. Soc. Chem. Commun.* **1976**, 600–601.
[6] W. E. Savige, A. Fontana, *Int. J. Pept. Protein Res.* **1980**, *15*, 102–112.
[7] a) J. P. May, P. Fournier, J. Pellicelli, B. O. Patrick, D. M. Perrin, *J. Org. Chem.* **2005**, *70*, 8424–8430; b) J. P. May, D. M. Perrin, *Chem. Eur. J.* **2008**, *14*, in press, DOI: 10.1002/chem.200701088.
[8] G. Shoham, W. N. Lipscomb, T. Wieland, *J. Am. Chem. Soc.* **1989**, *111*, 4791–4809.
[9] G. Zanotti, C. Birr, T. Wieland, *Int. J. Pept. Protein Res.* **1981**, *18*, 162–168.
[10] G. Zanotti, G. Dauria, L. Paolillo, E. Trivellone, *Biochim. Biophys. Acta Protein Struct. Mol. Enzymol.* **1986**, *870*, 454–462.
[11] G. Zanotti, G. Dauria, L. Paolillo, E. Trivellone, *Int. J. Pept. Protein Res.* **1988**, *32*, 9–20.
[12] G. Zanotti, G. Petersen, T. Wieland, *Int. J. Pept. Protein Res.* **1992**, *40*, 551–558.
[13] G. Zanotti, T. Wieland, E. Benedetti, B. Diblasio, V. Pavone, C. Pedone, *Int. J. Pept. Protein Res.* **1989**, *34*, 222–228.
[14] T. Wieland in *Peptides of Poisonous Amanita Mushrooms* (Ed.: A. Rich), Springer, New York, **1986**.
[15] N. N. Batada, K. D. Westover, D. A. Bushnell, M. Levitt, R. D. Kornberg, *Proc. Natl. Acad. Sci. USA* **2004**, *101*, 17361—17364.
[16] H. Boeger, D. A. Bushnell, R. Davis, J. Griesenbeck, Y. Lorch, J. S. Strattan, K. D. Westover, R. D. Kornberg, *Febs. Lett.* **2005**, *579*, 899–903.
[17] D. A. Bushnell, P. Cramer, R. D. Kornberg, *Proc. Natl. Acad. Sci. USA* **2002**, *99*, 1218–1222.
[18] D. A. Bushnell, R. D. Kornberg, *Proc. Natl. Acad. Sci. USA* **2003**, *100*, 6969–6973.
[19] D. A. Bushnell, K. D. Westover, R. E. Davis, R. D. Kornberg, *Science* **2004**, *303*, 983–988.
[20] P. Cramer, D. A. Bushnell, R. D. Kornberg, *Science* **2001**, *292*, 1863–1876.
[21] A. L. Gnatt, P. Cramer, J. H. Fu, D. A. Bushnell, R. D. Kornberg, *Science* **2001**, *292*, 1876–1882.
[22] D. Wang, D. A Bushnell, K. D. Westover, C. D. Kaplan, R. D. Kornberg, *Cell* **2006**, *127*, 941–954.
[23] K. D. Westover, D. A. Bushnell, R. D. Kornberg, *Cell* **2004**, *119*, 1055–1055.
[24] K. D. Westover, D. A. Bushnell, R. D. Kornberg, *Cell* **2004**, *119*, 481–489.
[25] K. D. Westover, D. A. Bushnell, R. D. Kornberg, *Science* **2004**, *303*, 1014–1016.
[26] Y. Arima, M. Nitta, S. Kuninaka, D. W. Zhang, T. Fujiwara, Y. Taya, M. Nakao, H. Saya, *J. Biol. Chem.* **2005**, *280*, 19166–19176.
[27] C. Casse, F. Giannoni, V. T. Nguyen, M. F. Dubois, O. Bensaude, *J. Biol. Chem.* **1999**, *274*, 16097–16106.
[28] C. Koumenis, A. Giaccia, *Mol. Cell. Biol.* **1997**, *17*, 7306–7316.
[29] G. Shoham, D. C. Rees, W. N. Lipscomb, G. Zanotti, T. Wieland, *J. Am. Chem. Soc.* **1984**, *106*, 4606–4615.
[30] T. Wieland, C. Gotzendorfer, J. Dabrowski, W. N. Lipscomb, G. Shoham, *Biochemistry* **1983**, *22*, 1264–1271.
[31] W. Schmitt, G. Zanotti, T. Wieland, H. Kessler, *J. Am. Chem. Soc.* **1996**, *118*, 4380–4387.
[32] K. L. Greenman, D. M. Hach, D. L. Van Vranken, *Org. Lett.* **2004**, *6*, 1713–1716.
[33] K. Baumann, G. Zanotti, H. Faulstich, *Protein Sci.* **1994**, *3*, 750–756.
[34] E. C. Kostansek, W. N. Lipscomb, R. R. Yocum, W. E. Thiessen, *J. Am. Chem. Soc.* **1977**, *99*, 1273–1274.
[35] E. C. Kostansek, W. N. Lipscomb, R. R. Yocum, W. E. Thiessen, *Biochemistry* **1978**, *17*, 3790–3795.
[36] S. F. Brady, S. L. Varga, R. M. Freidinger, D. A. Schwenk, M. Mendlowski, F. W. Holly, D. F. Veber, *J. Org. Chem.* **1979**, *44*, 3101–3105.
[37] E. Frerot, J. Coste, A. Pantaloni, M. N. Dufour, P. Jouin, *Tetrahedron* **1991**, *47*, 259–270.
[38] P. Li, P. P. Roller, J. C. Xu, *Curr. Org. Chem.* **2002**, *6*, 411–440.
[39] A. Ehrlich, H. U. Heyne, R. Winter, M. Beyermann, H. Haber, L. A. Carpino, M. Bienert, *J. Org. Chem.* **1996**, *61*, 8831–8838.

Received: August 22, 2007
Revised: November 12, 2007
Published online: February 28, 2008

